Scaling the Dynamics of Free-flight Wind Tunnel Models

Dhana E. Narayanasamy[1]

University of New South Wales at the Australian Defence Force Academy

UNSW Canberra has been running experiments to measure the aerodynamics coefficients and the external flow fields on free-flight models of high speed aerial vehicles in ground-based test facilities. It is found that the dynamic behaviour of the free flying models is a function of both the aerodynamics of the flow over the model and also the mass distribution of the model. A clear analytical model of the scaling of the dynamic behaviour is vital to both make sense of the measured dynamic response of the model and to select an optimum mass distribution of the model for an experiment. The shuttle orbiter was used as a candidate geometry for the scaling laws as it travels at hypersonic speeds. It was found that the scaling laws are in good agreement with real flight data. The ratio of air density between shuttle altitude to that at model altitude was an important factor when scaling the mass of the model. This affected the mass of the model and how the wind tunnel conditions are set. The altitude at which the shuttle orbiter experiments are carried out affected the sensitivity of the air density ratio.

Contents

Nomenclature

a	=	acceleration [m/s^2]
α	=	angular acceleration [rad/s^2]
c	=	chord [m]
C_m	=	pitching moment coefficient
D	=	drag [N]
Δd	=	displacement increment [m]
Δt	=	time increment [s]

[1] LT, School of Engineering & Information Technology, ZEIT4501

I_{yy} = moment of inertia, pitch [kg·m^2]
I = moment of inertia [kg·m^2]
L = lift [N]
ℓ = representative unit of length [m]
m = model mass [kg]
M = Mach no.
M' = moment [Nm]
N = model-to-airplane scale ratio
σ_r = ratio of air density at airplane altitude to that at model altitude
ρ = density [kg/m^3]
Q = pitch rate [rad/s]
q = dynamic pressure [Pa]
ω = angular velocity [rad/s]

Subscripts
A = full-scale aircraft
m = model
y = pitch axis

I. Introduction

The determination of aerodynamic coefficients has been a vital aspect of the aeronautics industry. Currently, three methods exist to determine the aerodynamic coefficients of an aircraft; full-scale flight tests, solving the aerodynamic coefficients using numerical simulations and wind tunnel testings. Wind tunnel testing is usually done using models attached to a sting to measure aerodynamic coefficients such as lift, drag and moment. However, with the sting attached to the model, either at the bottom or the rear of the model, some inaccuracies and discrepancies in the results obtained from the test due to flow interference from the sting. Free-flight wind tunnel tests are carried out by using small models in a wind tunnel without the support of a sting thus removing the flow interference. Also, with the use of a high-speed camera, you can capture the dynamic motion of the free-flight model and study its dynamic characteristics. In terms of the testing of hypersonic flows, the test flows are in the order of milliseconds. This is due to production of high enthalpy flow conditions in the shock tunnel which are of extremely short duration [1]. Hypersonic flows are classified as flows of $M \geq 5$. Therefore accurate modelling and proper selection of instrumentation are required.

II. Background

A. Aims

The aim of this project was to determine the scaling laws for hypersonic free-flight wind tunnel tests. These scaling laws were then used to validate existing experimental data and applied to additional candidate geometries.

The ideal project outcome would be that the scaling laws provide accurate modelling of free-flight models and they deliver accurate experimental results. The scaling laws that are determined via this project are to be applied to hypersonic experiments to determine its validity in the hypersonic area of study.

B. Aerodynamic Coefficients

An aircraft has four different forces that act on it; thrust, lift, drag and weight (gravity). Thrust forces the air to flow over the fuselage and wings, producing lift and drag forces. Drag is produced due to the viscous interaction between the air molecules and the surface of the aircraft as the air flows over the wings and the fuselage. Lift is produced by the air flow over the wings. This creates a low pressure region over the top part of the wing and a high pressure region under the wing. This phenomenon has a "sucking effect" on the wing causing a lift force.

Figure 1. Forces on an Aircraft

These lift and drag forces are dependent on a number of variables, such as the velocity of the aircraft, the dimensions of the aircraft, angle of attack, atmospheric variables and etc. Due to this large number of variables, any parametric or flow analysis carried out, requires each of these variables to be independently varied in order to obtain correct test data. By performing dimensional analysis, these aerodynamic forces can be then defined in terms of the dimensionless aerodynamic coefficients. This makes it easier to do calculation and also allows the tester to obtain the correct data [2]. The aerodynamic coefficients that will be looked into this project are, lift (C_L), drag (C_D) and moment (C_m).

$$C_L = \frac{L}{\frac{1}{2}\rho_\infty V_\infty^2 S} \qquad C_D = \frac{D}{\frac{1}{2}\rho_\infty V_\infty^2 S} \qquad C_m = \frac{M'}{\frac{1}{2}\rho_\infty V_\infty^2 Sc} \qquad \text{(1a, b, c)}$$

For the purpose of this project, the coefficient of moment (C_m) is the aerodynamic coefficient that is looked into mostly as it can determine the dynamic behaviour of a flying object.

III. Formulation of Scaling Laws

The formulation of the scaling laws was done via using the research paper by Scherberg and Rhode [3]. The research paper outlines the mathematics and theory of the scaling laws that are essential for free-flight testing and have been used in other various experiments. Though most free-flight testings are done for larger scale models and in a spin testing environment, these scaling laws are still applicable for wind tunnel testing.

A. Scaling Laws

When an airplane model is to be used for free-flight testing, it must be balanced dynamically and statically. Therefore, the model's mass distribution must be properly and accurately scaled. The model must not only have a given weight and a proper centre of gravity but also have a given ellipsoid of inertia [3]. Scherberg and Rhode [3] have come up with equations to show that a model, built with little regard to its mass distribution, may be loaded with masses of predetermined weight, shape, position and attitude to give the desired mass distribution. For models that are to be used in free-flight testing, the mass forces and the moments would greatly affect its performance. It is found that any motion may be considered to be made up of a series of steady helical motions which take place in infinitesimal time increments. Scherberg and Rhode [3] have defined that the mass distribution can obtained via two parts:

a. Obtaining the mass distribution for a steady helical motion, and
b. Proving the mass distribution in case (a) is satisfactory for any motion

B. Theory

Case (a) Mass Distribution for a Steady Helical Motion

The model must first be geometrically similar to the full-scale aircraft. Therefore, the model's linear dimensions must be N times those of the full-scale aircraft. N is the scale of the model. In order for the motions of both the full-scale aircraft and the model to be similar, the helix angles of homologous point paths must be equal. It is considered that the helical motion is obtained in a normal tail spin.

$$\frac{\ell_m}{\ell_A} = N \tag{2}$$

$$\frac{\omega_A \ell_A}{V_A} = \frac{\omega_m \ell_m}{V_m} \text{ or } \frac{\omega_A}{\omega_m} = \left(\frac{V_A}{V_m}\right) N \tag{3}$$

Since the aircraft is in a helical motion, the directions of the gravitational, centripetal and aerodynamic force vectors are similar and since the motion is steady, their resultants are equal to zero. Aerodynamic forces are proportional to $\ell^2 V^2$, gravitational forces are proportional to mass, and centripetal forces to $m\omega^2\ell$, thus giving the equations:

$$\frac{m_A}{m_m} = \frac{\ell_A^2 V_A^2}{\ell_m^2 V_m^2} \tag{4}$$

$$\frac{m_A \omega_A^2 \ell_A}{m_m \omega_m^2 \ell_m} = \frac{\ell_A^2 V_A^2}{\ell_m^2 V_m^2} \tag{5}$$

From equations (3), (4) and (5):

$$\omega_A = \omega_m \sqrt{N} \qquad V_A = V_m \Big/ \sqrt{N} \qquad m_A = m_m \Big/ N^3 \tag{6, 7, 8}$$

These equations establish the relationships between the angular velocity, linear velocity and the mass. The aerodynamic moment vector and the inertia couple vector are in the same direction when in a helical motion. Therefore, for the inertia couple and the aerodynamic moment to be in equilibrium in one plane of motion, the components of the resultant moments in all other planes must sum up to zero. This will satisfy all conditions of a steady helical motion. During steady motion, the inertia couple is a reaction couple due to forced rotation about an axis other than a principal one [3].

$$\frac{I_{pA}\omega_A^2}{I_{pm}\omega_m^2} = \left(\frac{\ell_A}{\ell_m}\right)^2 \left(\frac{V_A}{V_m}\right)^2 \left(\frac{\ell_A}{\ell_m}\right) \tag{9}$$

The left side of equation (9) is the ratio of the centrifugal couple while the right side is the ratio of the aerodynamic moments. The product of inertia is as stated in Figure 2. This corresponds to the moment components parallel to the '*ij*' plane. Using the relationships derived in equations (4) to (8), it is found that:

$$\frac{I_{pA}}{I_{pm}} = \frac{1}{N^5} \tag{10}$$

Thus the momental ellipsoid of the model at corresponding points must be similar in shape and parallel in attitude to that of the full-scale aircraft and have a linear scale ratio of N^5.

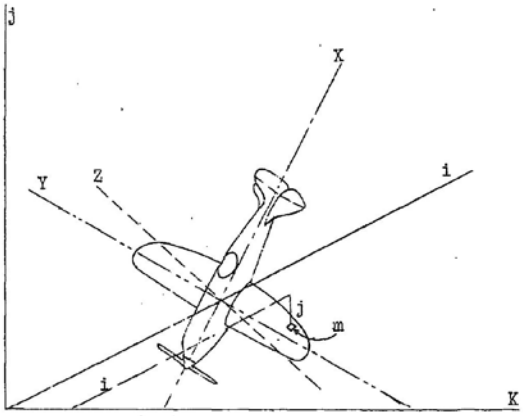

Figure 2. Product of Inertia, Ip=Σmij [3]

Case (b) Mass Distribution for any Motion

Assume at some instant, equation (4), (7) and (8) are true and the gravity vectors are similarly located for both model and the full-scale aircraft. Also the forces, and moments are similarly located thus the force and moment diagrams are similar. By equating the ratios of the vectors, we will see that:

$$\frac{F_A}{F_m} = \left(\frac{m_A a_A}{m_m a_m}\right) = \left(\frac{m_A g_A}{m_m g_m}\right) = \frac{1}{N^3}$$

$$\frac{F_A \ell_A}{F_m \ell_m} = \left(\frac{I_A \alpha_A}{I_m \alpha_m}\right) = \left(\frac{\alpha_A}{N^5 \alpha_m}\right)$$

$$\therefore \alpha_A = \alpha_m N \tag{11}$$

During the increments of time, the motion will be similar to the steady helical motions [3]. Therefore, the displacement increments of the mass particles will be:

$$\Delta d_m = N \Delta d_A \tag{12}$$

where the displacement can be linear or circular ($\ell\omega$). By dividing equation (12) by (6) and (7):

$$\sqrt{N}\,\Delta t_A = \Delta t_m \tag{13}$$

The new velocities, accelerations and positions at the end of the time intervals fulfil the conditions previously assumed [3].

$$V_A \Delta t_A = V_A + \Delta V_A = V_A + a_A \Delta t_A \tag{14}$$

$$V_A \Delta t_m = V_m + \Delta V_m = \sqrt{N} V_A + \sqrt{N}\, a_A \Delta t_A \tag{15}$$

hence,

$$\frac{V_A \Delta t_A}{V_A \Delta t_m} = \frac{1}{\sqrt{N}} \tag{16}$$

C. Summary of Scaling Laws

Using these scaling laws, the manoeuvres of a full-scale aircraft under the action of gravity alone can be completely simulated by a model if its mass quantity has been scaled to N^3. Also for the centre of gravity to be located at the same location as the full-scale aircraft, the model's centroidal ellipsoid, moment of inertia, must be scaled to N^5. However, this applies to incompressible flows. Since hypersonic flows are compressible, the area and moment of inertia factors have to be divided by σ_r, which is the ratio of air density at airplane altitude to that at model altitude [4]. The summary of scaling laws to be applied to a model:

Acceleration	a	$\boldsymbol{1}$
Geometry (*l, w, h*)	m	$\boldsymbol{N}$
Mass	kg	$\boldsymbol{N^3/\sigma_r}$
Area	m^2	$\boldsymbol{N^2}$
Moment of Inertia	kg/m^2	$\boldsymbol{N^5/\sigma_r}$
Linear Velocity (*v*)	m/s	$\boldsymbol{N^{0.5}}$
Angular Velocity (*ω*)	rads/s	$\boldsymbol{N^{-0.5}}$
Time	s	$\boldsymbol{N^{0.5}}$
Angular acceleration (*α*)	$rads/s^2$	$\boldsymbol{N^{-1}}$
Moment	Nm	$\boldsymbol{N^4}$

Table 1. Summary of Scaling Laws

IV. Shuttle Orbiter

A. Geometry/Theory

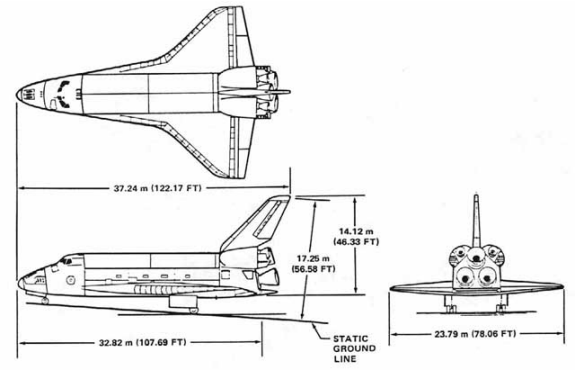

Figure 3. Shuttle Orbiter Dimensions [5]

Mass	*83001 kg*
Length	*37.24 m*
Width	*23.8 m*
Height	*17.25 m*
Chord	*12.06 m*
Reference Area	*249.91 m^2*
Centre of Gravity (X_{cg})	*0.65 to 0.675 x/L*
Centre of Pressure (X_{cp})	*0.65 x/L*
Moments of Inertia (Pitch)	*7 816 290 kg/m^2*

Table 2. Shuttle Orbiter Dimensions [5, 6]

The shuttle orbiter is chosen as the candidate geometry due to the fact that its flight regime involves speeds that are in the hypersonic region. Modified Newtonian Theory is used for the calculation of the forces and pressures that are present during the Shuttle Orbiter's flight. This is a simple form of looking into the forces involved which will help to calculate the pitching moment coefficient. Another reason for choosing the shuttle orbiter is due the fact that the shuttle orbiter has body flap. The body flap allows the centre of gravity (X_{cg}) to be properly trimmed to match the centre of pressure (X_{cp}). As specified in the Table 2, the X_{cg} is located between a range of 65 – 67.5 % of the body length of the shuttle orbiter from the nose [5]. This will allow me to check a range of C_m values for different values of the centre of gravity shift. The shuttle is modelled as a series of flat plates and the forces of each flat plate are calculated. After which they are integrated to give an overall value of the normal, lift and drag force.

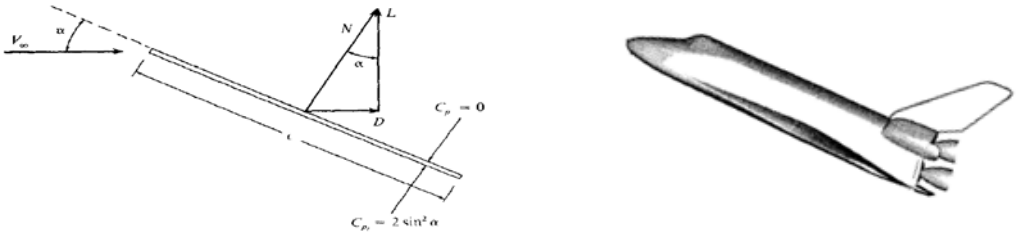

Figure 4. Newtonian Theory of Flat Plate vs Shuttle Orbiter [7]

The equations used are [7]:

$$N = \rho_\infty V_\infty^2 A \sin^2\theta$$

$$P = \frac{N}{A}$$

$$c_p = c_{p,\max} \sin^2\theta$$

$$c_n = c_{p,\max} \sin^2\theta$$

$$c_l = c_n \cos^2\theta$$

$$c_d = c_n \sin^2\theta$$

$$M_y = N \times \left(X_{cp} - X_{cg}\right)$$

$$c_m = \frac{M_y}{q \cdot S \cdot c} = \frac{I_{yy} \cdot \alpha}{q \cdot S \cdot c} \qquad \text{(17a-h)}$$

Though the shuttle is modelled as a flat plate, as seen in Figure 4, this can only be used as a crude estimation of the forces as the shuttle is not totally flat on the bottom. The curvature of the nose will result in some errors. However, since the curvature of the nose makes up only about 5% of the total length, I have assumed the shuttle orbiter to be flat throughout its length. A more detailed calculation involving the curvature of the nose will have to be considered in the future. The wings also have a curvature on the leading edges. Thus the same assumption of the nose is taken for the wings. Another assumption made in Newtonian theory is that the value of c_p is constant throughout the flat plate [7]. However, the shuttle being modelled as a series of flat plates, give different values of pressure as it's a function of area. This is then integrated to give the C_n and C_m values of the shuttle orbiter.

B. Results

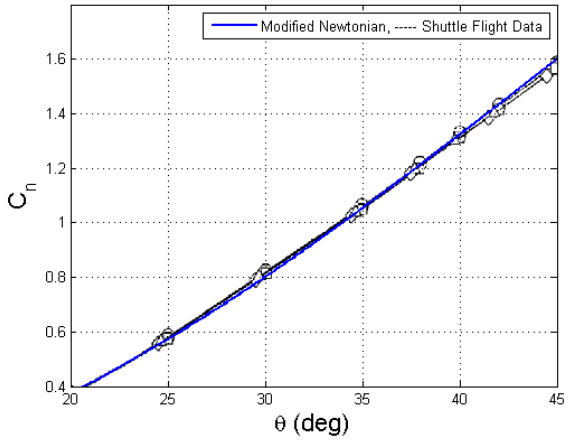

Figure 5. Normal Force Coefficient vs Angle of Attack

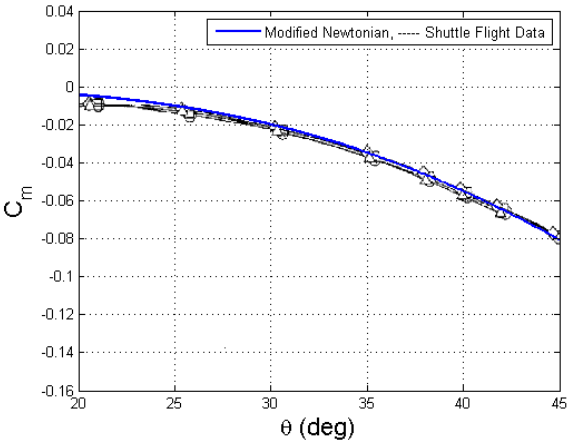

Figure 6. Pitching Moment Coefficient vs Angle of Attack

Using the scaling laws and the calculations above, an excel spreadsheet (Appendix A) and a MATLAB program was developed to see the trend of how different model scales will affect the pitching moment and the forces on the shuttle orbiter. The results were then compared with real flight data [8] of the shuttle orbiter to see if the scaling laws provide accurate data. To see if the Modified Newtonian theory calculation is able to model the space shuttle, the calculated C_n was plotted over a range of angles of attack and compared to real flight data.

Figure 5 shows that the calculation of the normal force coefficient is in good agreement with the real flight data of the shuttle orbiter [8]. Since the from the normal force coefficient we can calculate the lift, drag and moment of the shuttle, this will then result in an accurate calculation of the pitching moment coefficient.

The pitching moment coefficient was then calculated using the equations above and was plotted against the real flight data of the shuttle orbiter and it was noticed that at 20° angle of attack, the C_m value was -0.004 whereas the flight data was -0.01. This may be due to the fact that the nose is curved instead of being flat. However, as the angle of attack increased, the calculated data was in good agreement with the flight data. Both C_n and C_m plots showed that by using the modified Newtonian theory and modelling the shuttle orbiter as a series of flat plates, you are able to get accurate readings. A numerical analysis was carried out to the find out the normal, lift and drag forces for the shuttle orbiter. In Figure 7, L, which is the lift force, reaches a maximum value at about θ =55° and then begins to decrease. This is in relation with most hypersonic configurations [9].

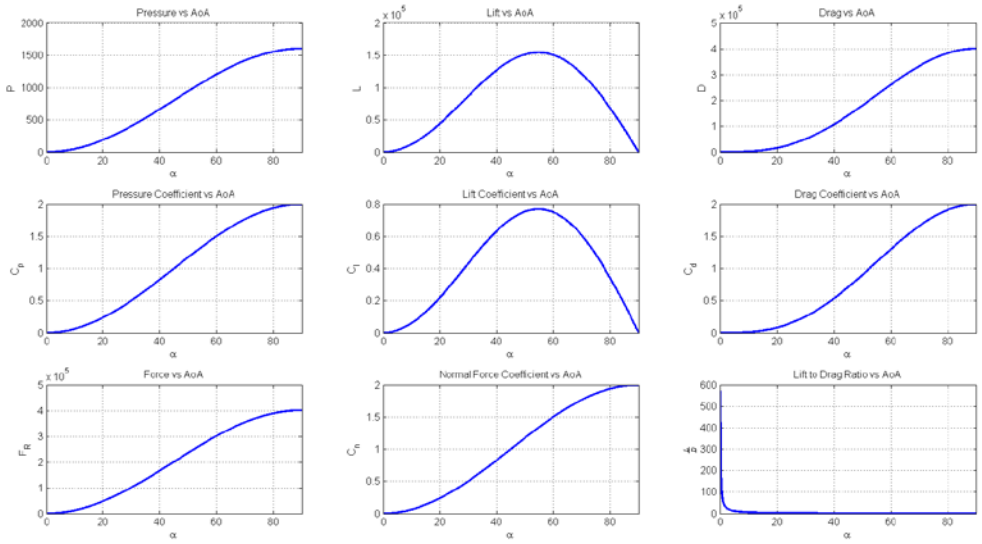

Figure 7. Numerical Analysis of Forces and Pressures for Shuttle Orbiter

Putting the scaling laws and the modified Newtonian theory calculations in a spreadsheet, I was able to see the trend of mass, velocity and moment values for different model scales of the shuttle orbiter. This was done to find a suitable model scale. It was found that, regards of scale, C_m was constant. This made sense as the scaling laws for all the other variables in the C_m formula are already scaled and thus the C_m should be constant.

$$C_m = \frac{M'}{\frac{1}{2}\rho_\infty V_\infty^2 Sc}$$

S is the reference area of the shuttle and it is scaled to N^2. c is the mean aerodynamic chord and it is scaled to N^1. V is the velocity and it is scaled to $N^{0.5}$. M' is the moment which is calculated using I_{yy} and α which are scaled N^5 and N^{-1} respectively. This then means that by correctly scaling all the other factors, the C_m should be constant whether it's the full scale aircraft or if it's a 1:200 scale model.

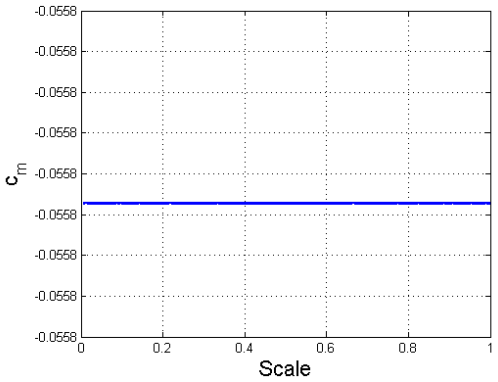

Figure 8. C_m vs Scale

$$C_m = \frac{M'}{\frac{1}{2}\rho_\infty V_\infty^2 Sc}$$

$$C_m = \frac{I_{yy} \times \alpha}{\frac{1}{2}\rho_\infty V_\infty^2 Sc}$$

$$C_m = \frac{N^5 \times N^{-1}}{N^{0.5} \times N^{0.5} \times N^2 \times N^1}$$

$$C_m = \frac{N^4}{N^4}$$

$$C_m = 1 \qquad (18)$$

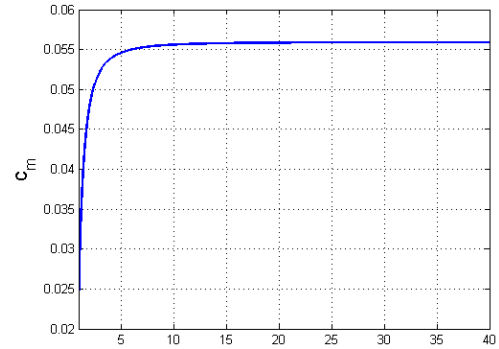

Figure 9. C_m Mach number dependence

When C_m is plotted against Mach number, it is found that C_m increases drastically when in the subsonic and supersonic region ($M \leq 4$). However, C_m starts to become constant at hypersonic speeds ($M \geq 10$) and only increases by 0.00001. Therefore it can be said that in a hypersonic flow, C_m is no longer dependent on the Mach number. This is true in theory because as the Mach number increases, the shock angle becomes steeper and reaches a point where it does not go pass the geometry. The shock is then parallel to the geometry and does not change as the Mach number increases [10]. For this case, this happens around Mach 10 therefore it is going to give the same C_m value even at Mach 20.

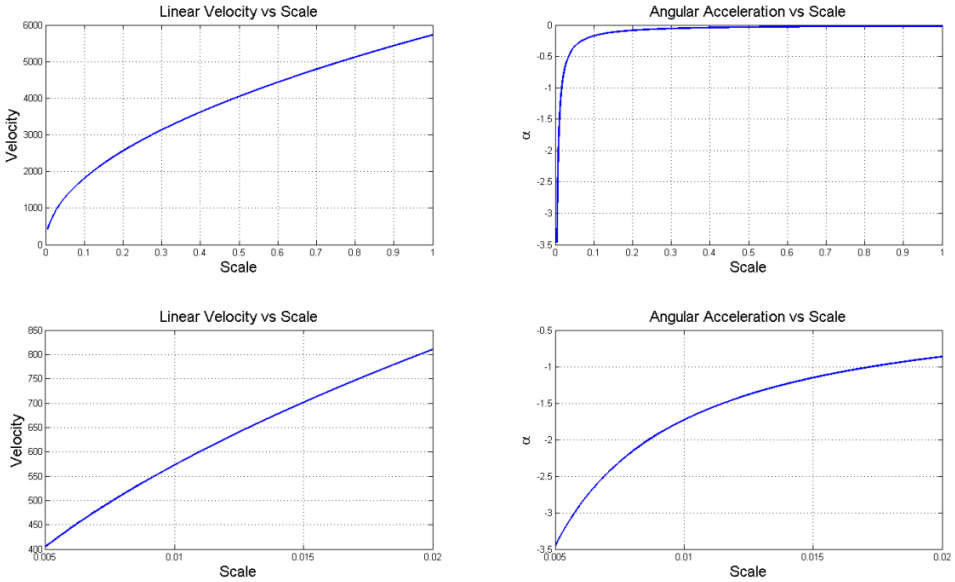

Figure 10. Velocity and Angular Acceleration Trends

Looking at the plots in Figure 10, we can see how the velocity and the angular accelerations change as the scale decreases. These plots were plotted with the assumption that the shuttle orbiter is at an altitude of 76km and with a speed of Mach 20. Scale 1 is the full scale aircraft and the scale 0.005 is a 1:200 scale model. For the model to mimic what the full scale aircraft does, it is noticed that the 1:200 scale model only needs to be flying at 405m/s and the angular acceleration is -3.46 rads/s^2. However the conditions in the wind tunnel have to be accurately set with Reynolds number and Mach number scaling to accurately simulate the conditions of the real flight. This will affect the density ratio of the air flow which is a key factor in scaling the mass of the model, which will be discussed in section C.

The reason for proper velocity and angular acceleration scaling is required is because these two variables are used in most of the calculations related to the Moment of the shuttle orbiter. Velocity is used to calculate the dynamic pressure which is used to calculate the aerodynamic coefficients. As displayed in Equation-17h, we can break up Moment about the pitch axis into the product of angular acceleration (α) and Moment of Inertia (I_{yy}). From the moment calculation, we can calculate the C_m. Also, with the data provided by the plots, appropriate instrumentation can be used to successfully capture the data from the model in the wind tunnel.

C. Mass of the Model

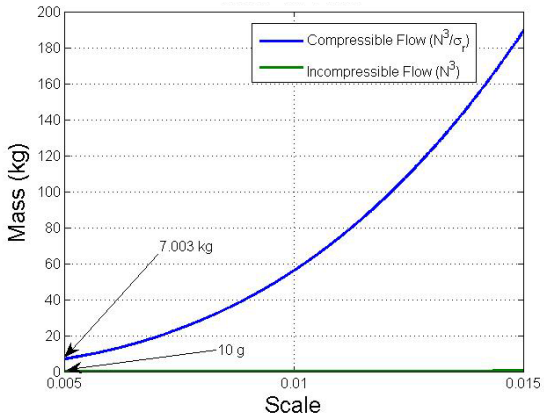

Figure 11. Compressible/Incompressible Mass Scaling

The mass of the model is the most important factor for the free-flight wind tunnel testing. As mentioned before, in order to accurately simulate the dynamic behaviour of a full scale aircraft in a wind tunnel, the mass of the model must be properly scaled. This however is governed by the density ratio between the air flow at which the full scale aircraft flies at and the air flow in the tunnel experienced by the model. This factor can be neglected for incompressible flows and the model needs to be scaled to N^3. But for hypersonic testing, the flow is compressible and the density ratio of the airflow plays a vital factor in the scaling of the model's mass, which is scaled to N^3/σ_r. Figure 11 shows the comparison between the differences in compressible in incompressible flows.

A full scale shuttle orbiter is 83001 kg. When this is scaled to N^3/σ_r, a 1:200 scale model will be 7 kg. This however depends on the atmospheric variables and also the density of the air flow at which the test is carried out at. For the purpose of this calculation, I have assumed that the shuttle is at an altitude of 76 km, which has an air density of 4.89 x 10^{-5} kg/m^3 and the air density of the test flow is 0.033 kg/m^3 [11]. 7 kg is heavy for a model but this can be adjusted by changing the flight conditions for the test and also the wind tunnel conditions. If the model's mass was scaled for an incompressible flow, then the model would have been 10 grams. This then

shows that the scaling of the mass is extremely sensitive to the density ratio of the air flow. A 10 g model will not be able to be tested in a shock tunnel as it will not be robust enough to withstand the strong shock wave that is produced in a shock tunnel. A 10 g model may not even reach the test section as it is too light.

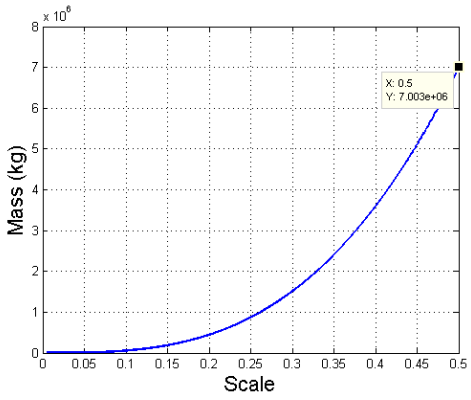

Figure 12. Mass rise due to scaling factor N^3/σ_r

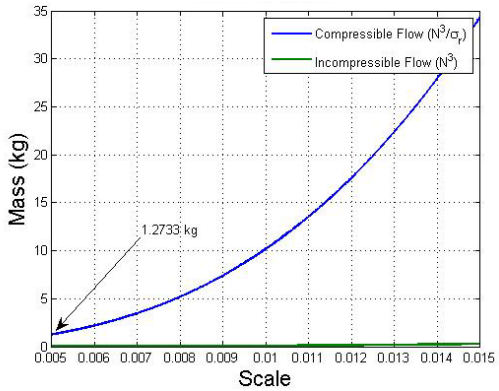

Figure 13. Mass vs Scale (T-ADFA conditions)

When the shuttle's mass is scaled to N^3/σ_r, it is noticed that there is a rise in the model's mass for bigger scales in terms of 10^3 kg. Figure 12 shows that for a 1:2 scale model, the mass of the model will be 7003050 kg. This again proves that the mass scaling is extremely sensitive to the density ratio and thus for testing bigger models, the tester has to consider the conditions at which the model is to be tested. Figure 13 shows if the model was tested in T-ADFA, with the air density condition specified as 0.006 kg/m^3 [12], the model will then have a mass of 1.2733 kg. This is a much acceptable weight for the model as it will be easier to fabricate.

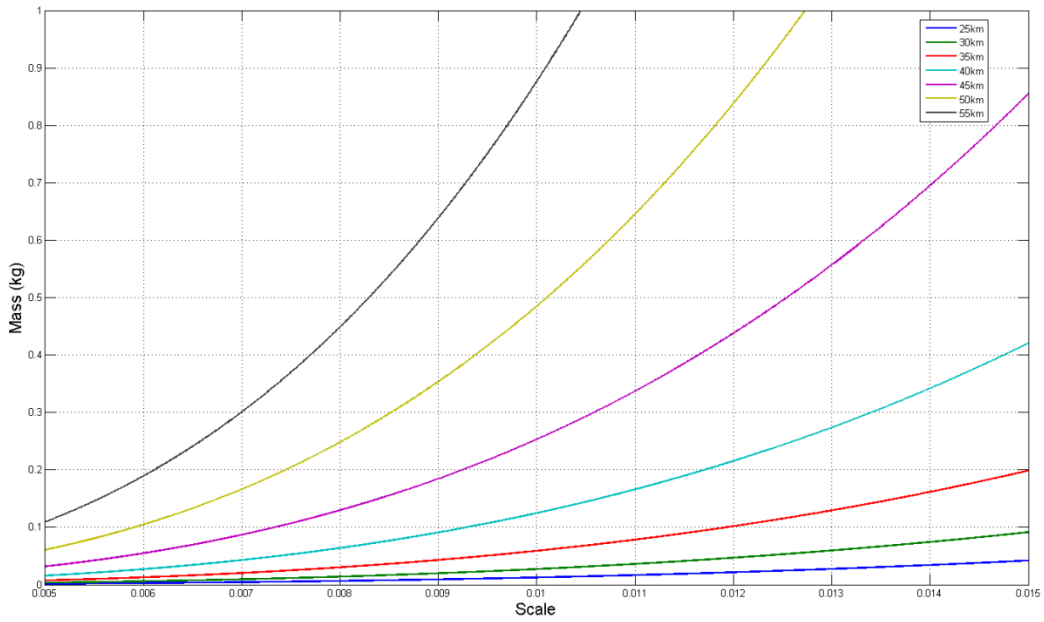

Figure 14. Altitude sensitivity due to N^3/σ_r scaling

To see the sensitivity of the density ratio in reference to altitude, the shuttle orbiter's mass was scaled to a range of altitudes from 25 km to 55 km in increments of 5 km. The test section density was set to condition B of T-ADFA with an air density 0.006 kg/m^3 [12]. As noticed in Figure 14, as the altitude increased, the mass of the model of a 1:200 scale model increased. As soon as the altitude decreased, the mass decreased drastically. A 1:200 scale model had a mass of 110 g at an altitude of 55 km (black line). But at 30 km altitude (green line), the mass was 3 g.

Hypersonic vehicles such as HEXAFLY operate at an altitude of 30 km [13] and are lighter than a shuttle orbiter. This means that the mass would be even lighter than 3 g for a generic hypersonic vehicle at a 1:200 scale. Therefore the conditions set in the shock tunnel must be calibrated to accommodate an acceptable model mass for the test or the full-scale aircraft's altitude must be set higher. This however will be the according to the tester's discretion. To calibrate the shock tunnel flow's air density is a tedious process. However it is possible to do so and the tester may have to consider modifying the full-scale aircrafts altitude.

V. Other Uses of Scaling Laws

The scaling laws can be used for other considerations such as material and instrumentation selection. With the mass scaling, the tester is able to pick an appropriate mass for the model. Knowing the mass of the model, the tester is able to choose the appropriate material for the fabrication of the model. This is important as the material has to be able to withstand the forces in the shock tunnel. The material has to be robust so that it does not get damaged during the test runs. The scaling laws that are used for the accelerations and velocities allow the tester to choose the appropriate instrumentations. Instrumentations such as accelerometers and gyroscopes are commonly used in free-flight testing. Using the scaling laws, the tester is able to deduce the range of accelerations and velocities that may be expected from the model and thus proper instrumentation can be chosen to capture the data from the test runs. Aircraft designers are able to use these scaling laws to fabricate a model and get data from them and with the data obtained, they are able to scale the model data to the full-scale aircraft.

VI. Future Work/Recommendations

This project has a lot of potential for future work. This project has solely been investigating the pitching rates and in the future, other dynamic behaviours such as roll and yaw rates may be looked into. Also the use of other candidate geometries maybe looked into. The proper calculation of the forces and moments is also another area that is vital for this project. As mentioned before, the shuttle orbiter was modeled as flat plate and this is only a crude estimation. Though the calculations were in good agreement with the flight data, to get an exact calculation, the nose bluntness and the curvature of the body needs to be taken into consideration. This is another area that can be considered for future development of this project. It is highly recommended that a model of the shuttle orbiter is fabricated with the scaling laws provided and tested in the shock tunnel for further validation.

VII. Conclusion

In conclusion, the project was successful in getting the scaling laws required for free-flight testing. It was found that, in order to have an accurate and reliable test data for free-flight wind tunnel tests, the model must not only be geometrically scaled but also dynamically scaled. Therefore, the mass scaling is vital when conducting such tests as it affects the dynamic behaviour of the model. The shuttle orbiter flight data was in good agreement with the data obtained from the scaling laws. It was shown how the ratio of air density, σ_r, was very sensitive to altitude changes and also how it affected the mass scaling. A proper shock tunnel and full scale altitude density had to be chosen for the accurate scaling of the mass. This then allows for proper fabrication of the model and acquisition of data. If the tester is unable to change the tunnel conditions, then the tester would have to consider changing the altitude density. The higher the altitude, which results to a lower density, made the mass of the model heavier. The mass of the model must be heavy enough to be able to withstand the flow of the shock tunnel. It was found that the pitching moment coefficient, C_m, remained constant regardless of scale. C_m was also independent of the Mach number at hypersonic speeds ($M \geq 5$).

VIII. Acknowledgements

I would like to sincerely thank my supervisor A/Prof. Andrew Neely for sacrificing his time in assisting me in this project. Without his guidance and knowledge, it would have not been possible to complete this project. I would like to thank Dr. Sean O'Byrne for his advice and knowledge in Hypersonics. I would also like to thank my fiancé, Ranjeeta Kaur for supporting and motivating me throughout my project. Finally I would like to thank my family and friends for believing in me.

References

[1] Neely, Andrew, Ivan West, Robert Hruschka, Gisu Park, and Neil Mudford. “Determining Aerodynamic Coefficients from High Speed Video of a Freeflying Model in a Shock Tunnel.” *28th International Congress on High-Speed Imaging and Photonics*, 2009.

[2] Nelson R.C, “Flight Stability and Automatic Control,” McGraw Hill, second edition, 1998

[3] Scherberg, M.; and Rhode, R.V.: "Mass Distribution and Performance of Free Flight Models," *NACA* TN 268, 1927.

[4] Wolowicz, Chester H., J. S. Brown Jr, and William P. Gilbert. "Similitude requirements and scaling relationships as applied to model testing." (1979).

[5] Bornemann, W. E., and T. E. Surber. "Aerodynamic design of the space shuttle orbiter." *1979. 24* (1979).

[6] Stone, Howard W., and Richard W. Powell. "Entry dynamics of space shuttle orbiter with lateral-directional stability and control uncertainties at supersonic and hypersonic speeds." (1977).

[7] Anderson, John David. *Hypersonic and high temperature gas dynamics*. Aiaa, 2000.

[8] Brauckmann, Gregory J., John W. Paulson, and K. James Weilmuenster. "Experimental and computational analysis of shuttle orbiter hypersonic trim anomaly." *Journal of Spacecraft and Rockets* 32.5 (1995): 758-764.

[9] Anderson, J. D. "Fundamentals of aerodynamics. 2001."

[10] Zel′dovich, I͡Akov Borisovich, Ya B. Zel’dovich, and Yu P. Raizer. *Physics of shock waves and high-temperature hydrodynamic phenomena*. Courier Dover Publications, 2002.

[11] Ennis, Rodney James. "ScramSpace hypersonic aerodynamic drag coefficient (CD) determined by free-flight experiments at TUSQ wind-tunnel." (2013).

[12] Choudhury, R., et al. "Hypersonic Drop-Tests of a Sphere: CFD Comparison to Experimental Results." (2010).

[13] Pezzella, Giuseppe, et al. "Aerodynamic Characterization of HEXAFLY Scramjet Propelled Hypersonic Vehicle."

Space Shuttle Model

Scale		1	2	3	4	5	6	7	8	9	10	20	50	100	150	200
Scale Factor of Full Size	N	1	1/2	1/3	1/4	1/5	1/6	1/7	1/8	1/9	1/10	1/20	1/50	1/100	1/150	1/200
Acceleration	a	5730.0	5730.0000	5730.0000	5730.0000	5730.0000	5730.0000	5730.0000	5730.0000	5730.0000	5730.0000	5730.0000	5730.0000	5730.0000	5730.0000	5730.0000
Length	m	37.2	18.6000	12.4000	9.3000	7.4400	6.2000	5.3143	4.6500	4.1333	3.7200	1.8600	0.7440	0.3720	0.2480	0.1860
Width	m	23.8	11.9000	7.9333	5.9500	4.7600	3.9667	3.4000	2.9750	2.6444	2.3800	1.1900	0.4760	0.2380	0.1587	0.1190
Height	m	17.3	8.6250	5.7500	4.3125	3.4500	2.8750	2.4643	2.1563	1.9167	1.7250	0.8625	0.3450	0.1725	0.1150	0.0863
Mass	kg	83001.0	1273281.8572	377268.6984	159160.2322	81490.0389	47158.5873	29697.5360	19895.0290	13972.9148	10186.2549	1273.2819	81.4900	10.1863	3.0181	1.2733
Area	m^2	249.9	62.4775	27.7678	15.6194	9.9964	6.9419	5.1002	3.9048	3.0853	2.4991	0.6248	0.1000	0.0250	0.0111	0.0062
Ivy (pitch)	kg/m^2	7816290.0	29976567.2939	3947531.4955	936767.7279	306960.0491	123360.3592	57074.4424	29273.9915	16244.9856	9592.5015	299.7657	3.0696E+00	9.59E-02	1.26E-02	3.00E-03
Linear Velocity (v)	m/s	5730.0	4051.7219	3308.2170	2865.0000	2562.5339	2339.2627	2165.7364	2025.8609	1910.0000	1811.9851	1281.2670	810.3444	573.0000	467.8525	405.1722
Angular Velocity (ω)	$rads/s$	-1.73E-02	-2.45E-02	-3.00E-02	-3.46E-02	-3.87E-02	-4.24E-02	-4.58E-02	-4.89E-02	-5.19E-02	-5.47E-02	-7.74E-02	-1.22E-01	-1.73E-01	-2.12E-01	-2.45E-01
Time	s	1.0	0.7071	0.5774	0.5000	0.4472	0.4082	0.3780	0.3536	0.3333	0.3162	0.2236	0.1414	0.1000	0.0816	0.0707
Angular acceleration (α)	$rads/s2$	-0.0173	-0.0346	-0.0519	-0.0692	-0.0865	-0.1038	-0.1211	-0.1384	-0.1557	-0.1730	-0.3460	-0.8650	-1.7300	-2.5950	-3.4600
Cp	m	24.1800	12.0900	8.0600	6.0450	4.8360	4.0300	3.4543	3.0225	2.6867	2.4180	1.2090	0.4836	0.2418	0.1612	0.1209
Cg	m	25.2960	12.6480	8.4320	6.3240	5.0592	4.2160	3.6137	3.1620	2.8107	2.5296	1.2648	0.5059	0.2530	0.1686	0.1265
r	m	-1.1160	-0.5580	-0.3720	-0.2790	-0.2232	-0.1860	-0.1594	-0.1395	-0.1240	-0.1116	-0.0558	-0.0223	-0.0112	-0.0074	-0.0056
c	m	12.0600	6.0300	4.0200	3.0150	2.4120	2.0100	1.7229	1.5075	1.3400	1.2060	0.6030	0.2412	0.1206	0.0804	0.0603
Moment	Nm	-1.352E+05	-8.451E+03	-1.669E+03	-5.282E+02	-2.164E+02	-1.043E+02	-5.633E+01	-3.301E+01	-2.061E+01	-1.352E+01	-8.451E+01	-2.164E-02	-1.352E-03	-2.671E-04	-8.451E-05
Cm	1	-0.0559	-0.0559	-0.0559	-0.0559	-0.0559	-0.0559	-0.0559	-0.0559	-0.0559	-0.0559	-0.0559	-0.0559	-0.0559	-0.0559	-0.0559

At 76200 m @ 40deg AOA

rho(actual)	4.89E-05	rho(test)	6.00E-03	rhorat Anm (σ_r) 8.15E-03
L=W=ma_N		a_N	9.5754	v=(2*pi*r)/t
ω = v/r				r=vt/2pi
I=mr^2				
cd	D/0.5*rho*v^2*S			
cl	L/0.5*rho*v^2*S			
cm	Ivy*α/qSl			

Inputs

scale factor